ORIGINAL PAPER

Dichromacy in the brown marmorated stink bug? Spectral sensitivity of the compound eyes and phototaxis of *Halyomorpha halys*

Ádám Egri[1] · Ádám Mészáros[1,2,3] · György Kriska[1,3] · József Fail[4]

Abstract

The brown marmorated stink bug (*Halyomorpha halys*) is an invasive pest insect species, which was recently introduced from Asia to America and then to Europe. Besides causing serious damage in agriculture, this species also represents a source of intense annoyance for humans in residential areas, because large amounts of individuals can aggregate on buildings while seeking shelter before overwintering. Taking into account the need for pesticide-free pest management methods, for example light trapping, we measured the spectral sensitivity of the compound eyes of *H. halys* with electroretinography (ERG). In behavioural experiments, we also quantified the attraction of *H. halys* to 14 quasi-monochromatic light stimuli in the 368–743 nm spectral range. The dark-adapted compound eyes were mostly sensitive to the green range, but a minor sensitivity peak in the UV region was also identified. Recordings on chromatic-adapted eye preparations unequivocally revealed the presence of only a green- and a UV-sensitive photoreceptor type, with sensitivity maxima at 519 nm and 367 nm, respectively. No sign of any blue-sensitive receptor was detected, and thus only a receptor set allowing dichromatic vision was found. Based on the results of the behavioural experiments, we established that the attraction of *H. halys* to light is increasing with decreasing wavelength, and thus we emphasize the importance of short wavelength lights (368–455 nm) when phototactic attraction of *H. halys* is the aim.

Key Message

- *Halyomorpha halys* is an invasive pest insect species, and little is known about its visual ecology.
- The sensitivity of the compound eyes is highest in the green spectral range.
- Electroretinography revealed two photoreceptor types, a green- and an ultraviolet-sensitive one.
- Attraction of *H. halys* to light is increasing with decreasing wavelength.

✉ Ádám Egri
  egri.adam@ecolres.hu

1   Centre for Ecological Research, Institute of Aquatic Ecology, Karolina út 29, Budapest 1113, Hungary

2   Doctoral School of Environmental Sciences, Eötvös University, Pázmány sétány 1, Budapest 1117, Hungary

3   Group for Methodology in Biology Teaching, Biological Institute, Eötvös University, Pázmány sétány 1, Budapest 1117, Hungary

4   Department of Entomology, Institute of Plant Protection, Hungarian University of Agriculture and Life Sciences, Ménesi út 44, Budapest 1118, Hungary

Introduction

The brown marmorated stink bug (*Halyomorpha halys* Stål, 1855) (Hemiptera: Pentatomidae) is an important, highly polyphagous invasive economic pest insect species (Vétek et al. 2018). It is native to Asia, primarily China, Korea and Taiwan (Hoebeke and Carter 2003; Lee et al. 2013), but it has been introduced also to America (Hoebeke and Carter 2003; Faúndez and Rider 2017) and recently to Europe (Haye et al. 2014). With around 300 reported hosts, this species represents a major threat to several agricultural and horticultural crops (Leskey et al. 2012a; Lee et al. 2013; Bariselli et al. 2016; Leskey and Nielsen 2018). The feeding

activity of *H. halys* causes direct damage to these plants (Leskey et al. 2012a; Lee et al. 2013; Rice et al. 2014), but it also transmits an Asian phytoplasma disease of the princess tree, *Paulownia tomentosa* (Leskey et al. 2012a).

Besides the serious problems caused in crop production, *H. halys* represents a significant source of annoyance in residential areas, because huge numbers of individuals often aggregate on buildings when they seek shelter and prepare for overwintering (Hancock et al. 2019).

The Integrated Pest Management (IPM) of *H. halys* in agricultural crop production includes various strategies that are using a monitoring tool for decision-making (Leskey and Nielsen 2018). Before the discovery of the aggregation pheromone of *H. halys*, this stink bug was monitored by using traps baited with methyl (2E, 4E, 6Z)-decatrienoate (MDT), the pheromone of the brown-winged green bug, *Plautia stali* Scott (Aldrich et al. 2007; Khrimian et al. 2008). After Khrimian et al. (2014) identified the two components of the male-produced aggregation pheromone of *H. halys* ((3S, 6S, 7R, 10S)-10,11-epoxy-1-bisabolen-3-ol and (3R, 6S, 7R, 10S)-10,11-epoxy-1-bisabolen-3-ol in a ratio of 3.5:1), traps used for monitoring were baited with the pheromone compounds and MDT, as the latter was found to increase trap catches in combination with the pheromone (Weber et al. 2014). Several trap designs and deployment strategies had been evaluated and ground deployed black pyramid traps were found to be more effective in capturing *H. halys* adults than small, limb-attached or hanging black pyramid traps deployed in crop canopy (Morrison et al. 2015) or transparent double-sided sticky traps (Acebes-Doria et al. 2020), although the latter has become more widespread in IPM decision-making as being more economic and just as reliable as the pyramid traps.

To reduce the environmental load caused by pesticides, alternative pest management methods, such as mass trapping are needed. The use of traps baited with aggregation pheromones often results in increased crop injury near the trap, since pests are attracted to the near vicinity of the baited trap but remain outside of the trap itself (this is often called as trap spillover). In order to utilize the above-mentioned traps as an effective pest management tool (mass trapping) rather than using them in decision-making, further development in the trapping of *H. halys* is needed. Improving knowledge about the behavioural ecology of *H. halys* could serve a basis for trapping development (Leskey and Nielsen 2018). Combining physical stimuli with olfactory stimuli could improve overall trap captures by bringing adult stink bugs together at close range and reducing spillover into the crop.

The potential use of substrate-borne vibrations for behavioural manipulation in order to interfere with pest behaviours and ultimately reduce crop damage has become evident in the last decade (Polajnar et al. 2015). The pair formation of stinkbugs, and in particular *H. halys*, is known to be

bimodal: it is based on the release of male-produced aggregation pheromones for long-range orientation followed by the emission of vibrational signals by females for short-range mating communication (Virant-Doberlet and Cokl 2004; Polajnar et al. 2016). Combining the aggregation pheromone with the female vibrational signal of *H. halys* improved trap catches under controlled and field conditions (Zapponi et al. 2022).

Visual stimuli are often used in insect trapping but incorporating visual cues into traps of *H. halys* has been generally overlooked, as little is known about the visual ecology of this insect species. Regarding the phototactic reactions of *H. halys*, it was shown initially that light traps can be used for monitoring (Nielsen et al. 2013; Lee et al. 2013). Afterwards, the attractiveness of non-monochromatic light sources to *H. halys* with different spectral characteristics were evaluated. It turned out that short-wavelength-dominated (UV and blue) light sources elicited high attraction but white light with UV content was the most attractive (Leskey et al. 2015; Cambridge et al. 2017). A recent study also demonstrated that a multimodal trap for *H. halys* can be very effective, especially when both UV-A and visible wavelengths are combined with pheromones (Rondoni et al. 2022). Besides the previously mentioned behavioural studies on *H. halys*, the spectral sensitivity of the compound eyes of the southern green stink bug *Nezara viridula* (Linnaeus, 1758), a close relative of *H. halys*, was also measured by Endo et al. (2014). Until now, this was the only case when the electroretinogram (ERG) of a stink bug was measured. Electroretinography is an electrophysiological method with which, for example, the spectral sensitivity of an insect eye can be measured (DeVoe et al. 1997). Endo et al. (2014) showed that the dark-adapted eye of *N. viridula* is mostly sensitive to the green, but a secondary sensitivity maximum is also present in the UV spectral range. They also tested the flight-to-light behaviour for some quasi-monochromatic wavelengths and found that attraction was highest for the UV and decreased with increasing wavelength.

To broaden our knowledge about the vision in the family of Pentatomidae we measured the spectral sensitivity of the compound eyes of *H. halys* with electroretinography, as well as the phototactic behaviour of this invasive species as a function of light wavelength.

Material and methods

Insects

H. halys individuals were collected from tree of heaven (*Ailanthus altissima*), ash-leaved maple (*Acer negundo*) and Norway maple (*Acer platanoides*) trees in the town of Zsámbék, Hungary (N 47.55239°, E 18.73243°) between 15

and 22 September 2021. This means that the collection was performed just before *H. halys* seek shelter for overwintering. The insects were kept in Bugdorm® cages at 21–23 °C under natural illumination. Red firethorn's (*Pyracantha coccinea*) fruit, apple, raw sunflower seed and green pods of common bean (*Phaseolus vulgaris*) were provided to the insects as food.

Electroretinography recordings

For ERG recordings each insect was laid upside down on a Plexiglas® piece with removed legs and was fixed to the Plexiglas® with a rubber band (Fig. 1). The measuring and the reference electrodes were composed of a cotton wick protruding from a pipette tip filled with 0.9% NaCl solution where a chloridized silver wire was also immersed. In the case of the measuring and reference electrodes, the silver wire was in direct contact with the custom built amplifier (Fig. S1) and the ground, respectively. The measuring electrode was touching the surface of the eye, while the reference electrode was placed on the stump of the legs. Data were recorded with the free Audacity 2.2.1 audio recording software (https://www.audacityteam.org) and a USB sound card (C-Media CM6206 chipset) modified for DC measurements. Since most sound cards include 16-bit analogue to digital converters, which are fast enough for electrophysiological recordings, it is possible to record the potential as a function of time with a properly modified sound card (Kecskeméti et al. 2021). The left audio channel was used to record the photoreceptor responses, while a reference signal was fed to the right channel. The reference signal indicated the presence of light stimuli and also enabled to calibrate the voltage level of the left channel. Data were recorded to a 16-bit

Fig. 1 ERG measurements on *H. halys*. **A** *H. halys* preparation with attached cotton wick electrodes. The light guide terminal is at the top of the image. **B** Examples for measured photoreceptor responses elicited by 496 nm light stimuli with logarithmically increasing intensity (2.1×10^{12} photons/cm^2/s $< I < 2.1 \times 10^{16}$ photons/cm^2/s; step = 0.5 log unit). Grey region shows the stimulus duration, while the pair of dotted lines represents the 150-ms-long period, in which the response amplitudes were obtained
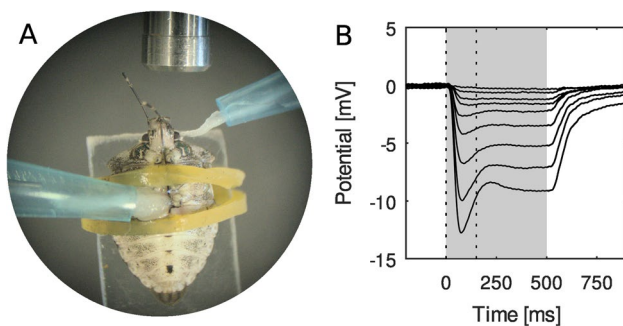
WAV audio file with a sampling frequency of 8 kHz. The linearity of the sound card inputs was checked and verified.

For delivering light stimuli to the eye preparations, a LED-based, custom-built and custom-calibrated light source was used, being able to create quasi-monochromatic light stimuli with variable light intensity (for details, see Egri and Kriska (2019)). In our measurements we used the following wavelengths (± half bandwidth of LED): 346 nm (± 5.0 nm), 376 nm (± 4.8 nm), 402 nm (± 5.5 nm), 421 nm (± 6.4 nm), 442 nm (± 8.5 nm), 467 nm (± 10.4 nm), 496 nm (± 13.5 nm), 516 nm (± 14.5 nm), 552 nm (± 17.7 nm), 598 nm (± 6.9 nm), 623 nm (± 7.7 nm), 641 nm (± 8.6 nm).

During recording, a series of 500-ms-long light stimuli was delivered to the eye preparation. The stimulus series consisted of 2–4 repetitions of the same sequence. In each sequence, the order of wavelengths was first increasing and then decreasing. For each wavelength, light stimulation was logarithmically increasing in intensity (intensity step was approximately 0.5 log unit) and the inter-stimulus intervals were 6 seconds long. When wavelength was switched, 12-s-long inter-stimulus interval was used. Photon flux of the applied light stimuli was between 2.0×10^{12} and 2.1×10^{16} photons cm^{-2} s^{-1}.

Four kinds of measurements were performed on female and male *H. halys* individuals: (i) Dark-adapted, (ii) green-adapted, (iii) UV-adapted, and (iv) UV-green-adapted. In the dark-adapted case, the eye preparations were kept in darkness before the recordings for 45 min. For chromatic adaptation, a green (λ_{peak} = 562 nm) and UV (λ_{peak} = 377 nm) LED was used (see emission spectra in Fig. S2). The photon flux of each adapting light was 1.4×10^{14} photons cm^{-2} s^{-1} at the eye preparation. The optical axis of the light guide and the direction of the adapting light formed an angle of approximately 30°. In the case of chromatic adaptations, a dark-adapted eye preparation was exposed to the adaptation light for 15 min prior to the recording. The exact type of the adapting LEDs was unknown, but their emission spectrum was calibrated with an Ocean Optics STS-VIS spectrometer (Ocean Optics, Largo, USA). The purpose of recordings performed on chromatic-adapted eyes was to reveal the photoreceptor set of *H. halys*. Chromatic adaptation is a method for extracellularly revealing the presence of different photoreceptor classes in the eye (Telles et al. 2014).

Photoreceptor response amplitudes were extracted from the recorded data by taking the magnitude of the negative potential jump in the first 150 ms of each light stimuli. For each wavelength, all response amplitudes were plotted against log stimulus intensity and Naka-Ruhston function (Naka and Rushton 1966; Skorupski and Chittka 2010) was fitted on the data. Spectral sensitivity was obtained by taking, wavelength-by-wavelength, the reciprocal of photon flux needed for eliciting a standard response criterion (20% of the maximal response amplitude for the given eye preparation).

Finally the spectral sensitivity was normalized with the value at 516 nm.

Altogether spectral sensitivity of 16 dark-adapted, 6 green-adapted, 6 UV-adapted and 6 UV-green-adapted eye preparations were measured. Number of measured females and males were equal in all cases.

Because all kinds of measurements resulted in bimodal spectral sensitivity curves possessing a UV and a green sensitivity maximum, the sum of two A1-based pigment templates (see Eqs. 1–5 in Govardovskii et al. (2000)) was fitted on the mean spectral sensitivity curves, except for the UV-adapted case, for which a single template was fitted on the data. The downhill simplex method (Nelder and Mead 1965) was used to fit the free parameters (λ_{max} and a vertically scaling factor for each pigment template) of the curves.

Behavioural experiments

Attraction of *H. halys* to light as a function of wavelength was measured in a series of behavioural tests in the 368–743 nm range. The experimental arena was a 50 cm × 25 cm × 25 cm (length × width × height) box lined with matte black cardboard (Fig. 2). At one terminal of the arena a custom-made light source was placed. From the other arena terminal, the test insects were released and their behaviour was recorded under 940 nm illumination with a webcam modified for infrared sensitivity.

The light source was a custom-built and custom-calibrated one, very similar to that of Egri et al. (2020). A LED array was fixed under a PVC elbow that was lined with aluminium foil (Fig. 2A, B). The array of LEDs consisted of 14 quasi-monochromatic LEDs with the following wavelengths (± half bandwidth of LED): 368 nm (± 6.8 nm), 389 nm (± 5.9 nm), 400 nm (± 6.4 nm), 423 nm (± 8.1 nm), 436 nm (± 8.3 nm), 455 nm (± 12.7 nm), 469 nm (± 11.1 nm), 497 nm (± 14.5 nm), 517 nm (± 17.3 nm), 552 nm (± 18.2 nm), 596 nm (± 7.9 nm), 630 nm (± 8.6 nm), 665 nm (± 10.4 nm) and 743 nm (± 11.0 nm). The light intensity of each LED was controlled with pulse width modulation (PWM) with a frequency of $f_{pwm} = 490$ Hz. Thanks to the aluminium foil lining of the PVC elbow and a piece of sandblasted glass at the upper elbow terminal, a circular (diameter = 10.6 cm), homogeneously illuminating surface represented the light stimulus for the test insects (Fig. 2C).

Before each trial, a specimen was placed 8 cm from the darker arena terminal (the light source was at the other terminal) on the mid-line of the arena under a convex clock glass (diameter = 8 cm) (Fig. 2A). The trial started with turning on the light stimulus. After 5 s, the insect was released by manually removing the clock glass, and 60 photographs (8-bit greyscale) were taken by the webcam with a rate of 1 frames per second (Fig. 3). Thus, one trial was exactly 60 s long. The darker arena terminal was the only part of
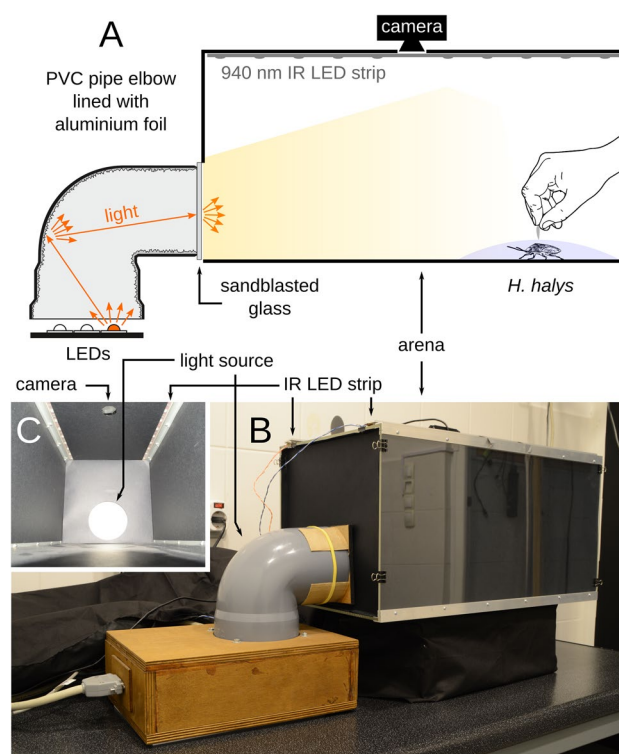

Fig. 2 Experimental set-up for the behavioural experiments. **A** Schematic diagram of the arena. **B** Photograph of the set-up. **C** Interior of the arena from the aspect of a test insect at the release point

the arena without a wall. This enabled the experimenter to manually remove the clock glass; however, the insects could leave the arena there. Insects were dark adapted for at least 90 min before the trials. Experimental blocks consisting of trials with the 14 wavelengths plus a dark control trial were performed in series. Four different intensities were used (7.68×10^{14}, 7.68×10^{13}, 7.68×10^{12} and 7.68×10^{11} photons cm^{-2} s^{-1}), but the applied stimulus intensity was constant throughout an experimental block (except for the control trial with no light). Numbers of blocks corresponding to a given intensity were equal ($n = 14$). On one day, typically 3 experimental blocks were made, and trials were performed at 20–22 °C and 50–55% relative humidity. In a total number of 56 experimental blocks 15 (trial types) × 14 (repetitions) × 4 (stimulus intensities) = 840 *H. halys* individuals were tested.

For a given trial, the position of the test insect was extracted from each photograph in pixel units with a custom-written software. In short, the median image of all 60 frames was calculated and was subtracted from each frame. Resultant pixel intensities having negative values were multiplied with -1, and finally a thresholding algorithm was applied (see also Fig. 1 D–H in Kecskeméti et al. (2021)). The threshold value was adjusted manually; however, in most of the cases the value of 10 was appropriate. It is also important to mention that sometimes, for example when the insect was
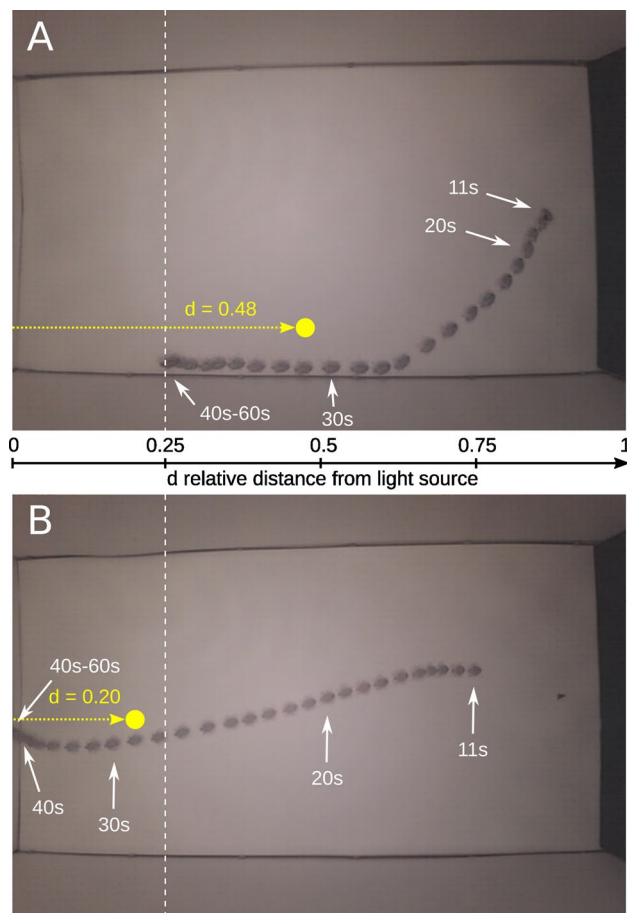
Fig. 3 Evaluation of the webcam images of the behavioural experiments. **A** The image is the minimum of images taken from the 11th second during a trial ($\lambda = 596$ nm, $I = 7.68 \times 10^{14}$ photons cm^{-2} s^{-1}). For demonstration purposes, calculating the minimum image was appropriate because the stink bugs were darker than the background. White vertical dashed line shows the critical relative distance of 0.25 measured from the light source. Yellow filled circle displays the centroid of the insect between the 11th and 60th seconds of the trial. Because the horizontal coordinate of the centroid is greater than 0.25, this insect was treated as inactive. **B** Same as **A** for another stimulus ($\lambda = 630$ nm, $I = 7.68 \times 10^{12}$ photons cm^{-2} s^{-1}). Here, the distance of the centroid from the light source terminal was smaller than 0.25, and thus the reaction of the insect was recorded as a positive phototactic choice

stationary for more than 30 s, the set of frames for calculating the median image was modified to avoid the presence of the specimen on the median image. In the most drastic cases, when the insect was not moving throughout the trial, the median image of another trial was used.

The horizontal coordinate of the insect was averaged for the last 50 frames of the trial (Fig. 3). The first 10 frames were not used to give some seconds for the insects to react. If the distance between this mean horizontal coordinate and the light source was less than 25% of the arena length, the choice of the test insect was treated as a positive phototactic

choice (Fig. 3B). In all other cases, the insect was regarded as inactive (Fig. 3A). Because sometimes the insect left the field of view of the camera (e.g. climbed on the wall or left the arena), the final position of the insect was manually recorded as one of these categories: (i) light source terminal: the insect was exactly on the arena terminal were the light source was; (ii) light source half: the insect was in the brighter half of the arena; (iii) dark half: the insect was in the darker half of the arena; (iv) dark terminal: the insect left the arena on the dark side. For these categories when the insect was not visible on the last frame, the final horizontal coordinates, measured in arena length units from the light source, were considered as 0, 0.25, 0.75 and 1, respectively. In the time interval(s) when the insect was not detected, the horizontal coordinate was linearly interpolated.

The numbers of flight attempts for all wavelengths and the dark control trials were also registered. Test insects tried to take off typically once. If not, only the first attempt was registered for the given trial.

Statistics

In the case of the dark-adapted measurements, the relative spectral sensitivity of the females and males was compared wavelength by wavelength with Mann–Whitney U tests. Similarly, Mann–Whitney U tests were used to compare the relative spectral sensitivity of the UV- and green-adapted eye preparations. In the case of behavioural experiments, the number of positive choices and inactive individuals was compared with χ^2 tests, wavelength by wavelength. For these χ^2 tests, the expected number of active and inactive individuals was taken from the corresponding values of the dark, control trials, when the light source was off. Statistical tests were performed with GNU Octave 6.4.0 and R 4.1.2 (R Core Team 2022). Although four different light intensities were used for each wavelength, we pooled together all data for a given wavelength, because the application of a given stimulus intensity was not randomized throughout the 5-week-long measurement campaign.

Results

Electroretinography recordings

Mean spectral sensitivity of the dark-adapted *H. halys* eye preparations is shown in Fig. 4. Sensitivity curves of females and males are indicated with grey and black colour, respectively. Vertical bars denote standard deviation. The solid curve is the fitted sum of two A1-based pigment templates (Govardovskii et al. 2000) displayed by dotted and dashed curves. Mann–Whitney U tests revealed no significant difference between the sensitivity of females and males at $\alpha = 0.05$
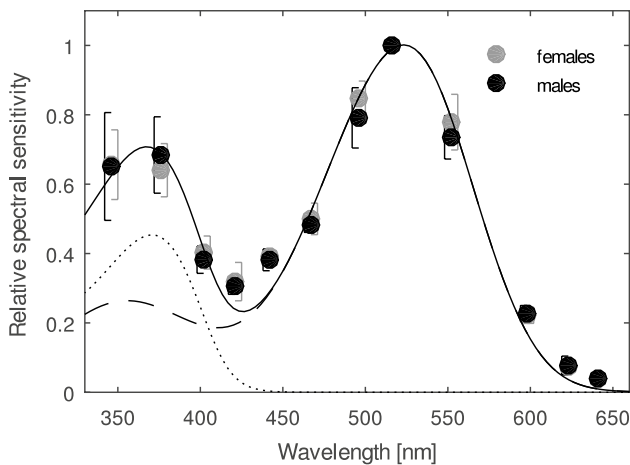
Fig. 4 Mean relative spectral sensitivity of 8 female and 8 male dark-adapted *H. halys* eye preparations. Grey and black dots show the data of females and males, respectively. Vertical bars denote standard deviation. Dashed and dotted curves show the fitted A1-based pigment templates (Govardovskii et al. 2000) of the green- and UV-sensitive photoreceptors, respectively. The solid curve is the fitted sum of these two templates. All curve fittings were performed on the pooled data of females and males

significance level. It is clear that the spectral sensitivity has a global maximum in the green range, and a secondary maximum in the UV region. The peak wavelength of each fitted pigment template was $\lambda_G^{dark} = 523$ nm and $\lambda_{UV}^{dark} = 371$ nm.

Figure 5 shows the mean relative spectral sensitivity curves of the chromatic-adapted eye preparations. Because the relative spectral sensitivity of dark-adapted females and males were statistically similar (Fig. 4), we pooled together the data of females and males for the chromatic-adapted cases. The concept of the fitted curves in Fig. 5 is the same as that of Fig. 4; however, in the UV-adapted case (Fig. 5B), only one A1-based Govardovskii template was fitted. When the eyes were green-adapted, a striking relative increase in UV sensitivity occurred (Fig. 5A) compared to the sensitivity curve of the dark-adapted preparations (Fig. 4). Peak wavelengths of the fitted templates were $\lambda_{UV}^{green} = 367$ nm and $\lambda_G^{green} = 519$ nm for the green-adapted case. Note that all curves are normalized with the value at 516 nm. On the other hand, when the eyes were adapted to UV light, the relative UV sensitivity was decreased (Fig. 5B) compared to the dark-adapted case (Fig. 4). Here the sensitivity maximum of the fitted pigment template was at $\lambda_G^{ultraviolet} = 519$ nm. These results are doubtless indications of distinct UV- and green-sensitive photoreceptors. Wavelength-by-wavelength statistical comparison of relative spectral sensitivity of green- and UV-adapted eye preparations with Mann–Whitney *U* tests revealed significant differences for the 346–421 nm wavelength range ($\alpha = 0.05$). Applying simultaneous UV and green adapting light resulted in qualitatively similar mean relative sensitivity curve (Fig. 5C, $\lambda_{UV}^{ultraviolet+green} = 374$ nm,
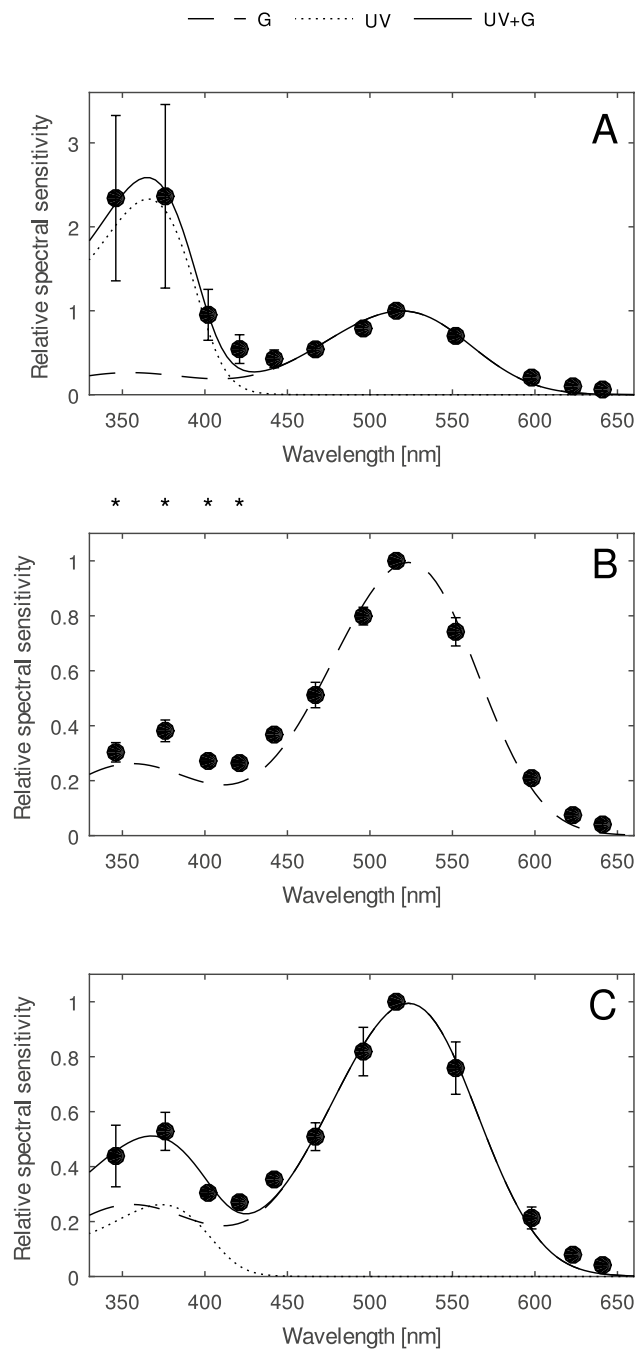

Fig. 5 Mean relative spectral sensitivity of chromatic-adapted eye preparations. **A** green-adapted, **B** UV-adapted and **C** UV-green-adapted case. Vertical bars indicate standard deviation. Description of the fitted curves is the same as given for Fig. 4. Asterisks between **A** and **B** show significant differences between the UV- and green-adapted cases revealed by Mann–Whitney *U* tests performed wavelength-by-wavelength (at $\alpha = 0.05$ significance level)

$\lambda_G^{ultraviolet+green} = 523$ nm) as obtained for the dark-adapted preparations (Fig. 4).

None of the chromatic-adapted ERG recordings resulted in the emergence of a sensitivity peak in the blue spectral range.

Behavioural experiments

Figure 6 shows the results of the behavioural phototaxis choice experiments. In Fig. 6A, the number of choices of *H. halys* individuals can be seen as a function of wavelength. Grey and black bars indicate the numbers of insects that chose the light source's side of the arena and the numbers of inactive insects, respectively. On the right, outside of the graph, the choices are displayed for the control trials, when the light source was off. The most important message of this graph is that the attraction of *H. halys* to light is increasing with decreasing wavelength. According to χ^2 tests, all
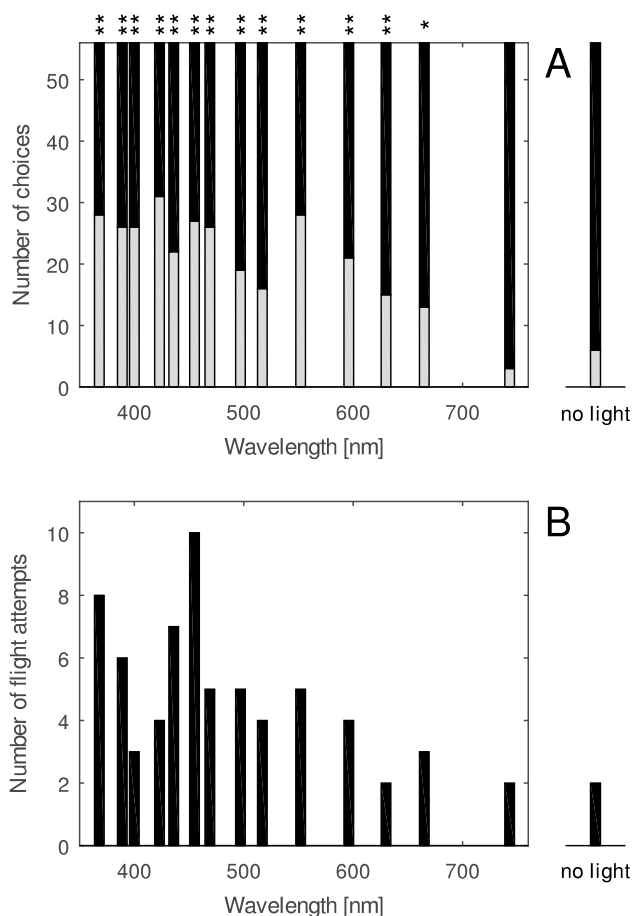
Fig. 6 Responses of *H. halys* to quasi-monochromatic stimuli in the behavioural experiment. **A** Number of choices as a function of wavelength. Grey bars represent positive phototactic choices, while the black bars show the numbers of inactive individuals. Asterisks at the top indicate whether the choices significantly differed from the expected choice numbers taken from the control trials. (*$p < 0.05$; **$p < 0.001$). **B** Number of flight attempts as a function of wavelength

wavelengths elicited a significant positive phototactic reaction, except for the 743 nm infrared light.

Figure 6B shows information exclusively about the flight behaviour of the test insects as a function of wavelength. The highest number of flight attempts was registered for 455 nm, but 368 nm was also attractive. In general, the attractiveness again increased with decreasing wavelength, however, a definite local minimum in attractiveness occurred around 400 nm.

Discussion

For the spectral sensitivity of dark-adapted *H. halys* preparations we obtained practically the same results as measured by Endo et al. (2014) for the close relative, *N. viridula*. They assumed that *N. viridula* has three types of photoreceptors (UV, blue and green), and thus they fitted the sum of three A1-based pigment templates on their data to estimate the sensitivity peak of the individual receptors. The contribution of the supposed blue-sensitive pigment in their curve fitting was relatively small. In our case for *H. halys*, the chromatic adaptations explicitly revealed the presence of only two distinct photoreceptor types, a UV- and a green-sensitive one. This was the reason for fitting the sum of no more than two A1-based pigment templates on our data. Thus, we suggest that if there is colour vision in *H. halys*, it is a dichromatic system, which might be true for other members of the family Pentatomidae, like *N. viridula*. It is also important to mention that we could not prove the lack of the blue receptors, and we could just state that we did not detect any. This is congruent with the lack of blue-sensitive opsin genes and the presence of long wavelength-sensitive opsin homologs and a UV-opsin homolog in the genome of *H. halys* (Sparks et al. 2020).

When the eyes were green-adapted, the sensitivity of the green-sensitive receptors was suppressed, and thus the sensitivity curve of the compound eye below 400 nm was dominated by the sensitivity of the UV-sensitive receptors. In other words, the contribution of the secondary absorbance peak (β-peak) of the green-sensitive receptors was minimized. Hence, we consider $\lambda_{UV}^{green} = 367$ nm as the position of the sensitivity maximum of the UV-sensitive receptors. Similarly, we suggest $\lambda_{G}^{ultraviolet} = 519$ nm for the sensitivity maximum of the green-sensitive receptors, because the contribution of the UV-sensitive receptors was minimized when the eyes were adapted to UV light.

Having only two receptor types is not uncommon in insects. Although dichromacy is usually found in ocelli (van der Kooi et al. 2021), there are certain species with compound eyes possessing two types of photoreceptors. For example, intracellular recordings revealed only UV- and green-sensitive photoreceptors in the compound eyes of the

Periplaneta americana (Linnaeus, 1758) and *Blatta orientalis* (Linnaeus, 1758) cockroaches (Mote and Goldsmith 1970; Mazokhin-Porshnyakov and Cherkasov 1985). Only UV and green-sensitive receptors were also found in the eyes of the beetle *Lethrus apterus* (Laxmann, 1770) (Gribakin 1981), as well as in the red flour beetle, *Tribolium castaneum* (Herbst, 1797) (Jackowska et al. 2007).

Colour vision requires at least two types of photoreceptors with appropriate neuronal interactions (van der Kooi et al. 2021). The presence of more than one photoreceptor type does not necessarily involve colour vision. In the behavioural experiments, we simply quantified the attraction to light as a function of wavelength, and we did not test whether *H. halys* possesses true colour vision. Future studies should test it because host plants of *H. halys* often have colourful fruits (Leskey et al. 2012a; Lee et al. 2013; Bariselli et al. 2016; Leskey and Nielsen 2018). The results of our ERG measurements performed on chromatic adapted preparations indicate that *H. halys* has a photoreceptor set allowing only dichromatic colour vision. In view of the fact that *H. halys* is strongly attracted to UV-including white light (Leskey et al. 2015; Cambridge et al. 2017), the reason for the attraction peak in the flight-to-light behaviour in the blue 436–455 nm range (Fig. 6B) might be caused by the simultaneous excitement of the UV and green receptors. According to a recent study, *N. viridula* is mostly attracted to UV, but attraction is enhanced when green is added (Endo et al. 2022). The reason for this may lie also in the simultaneous excitement of the two receptor types. Nevertheless, the most important output of our behavioural experiments is that the attraction is increasing towards shorter wavelengths. Thus, we emphasize the importance of short wavelengths (368–455 nm) for attracting *H. halys* individuals when monitoring or light trapping is the goal. Field tests are needed to assess to what extent spillover to the crop is reduced when short wavelength (368–455 nm) quasi-monochromatic visual stimuli are combined with pheromones in traps. Positive results from such field tests and the development of trap bodies that facilitate the capture of *H. halys* individuals in large numbers as well as the easy removal of the trapped bugs could potentially lead to efficient mass trapping of this economically significant pest and eventually reduce the reliance on pesticides in managing *H. halys*.

However, a number of field and laboratory studies reported that *H. halys* is generally attracted by light (Nielsen et al. 2013; Lee et al. 2013; Endo et al. 2014; Leskey et al. 2015; Cambridge et al. 2017; Rondoni et al. 2022), in certain cases, individuals were shown to be attracted by dark objects (Toyama et al. 2011; Leskey et al. 2012b). Our behavioural experiments showed that *H. halys* possesses positive phototaxis for all sensed wavelengths. Because we performed our experiments in autumn, we suggest that the considerable annoyance caused for humans when *H. halys* seek shelter before overwintering is most likely caused by the attraction to the artificial lights falling from windows of buildings after sunset. On the other hand, the heat dissipating from the buildings could also be attractive for *H. halys*, but it is not clear whether remote thermal sensing (Schmitz et al. 2012) or conventional thermoreception (Gingl et al. 2005) or both is used by *H. halys*. In several species of *Aradus* (Heteroptera, Aradidae), infrared receptors have been found (Schmitz et al. 2010). These pyrophilous insects feed on fungi that grow on burnt wood, and they use their specialized infrared-sensitive organs for remotely detecting fire. Besides studying the colour vision of *H. halys*, an extremely interesting research would be to test whether the brown marmorated stink bug possesses and uses infrared-sensitive organs when they search for shelter during the chilly autumn days.

Author contributions

ÁE contributed to conceptualization, funding acquisition, investigation, methodology, software, supervision, visualization, writing–original draft and writing–review and editing; ÁM contributed to investigation and writing–original draft; GK contributed to supervision and writing–review and editing; JF contributed to funding acquisition, supervision, writing–original draft and writing–review and editing. All authors gave final approval for publication and agreed to be held accountable for the work performed therein.

Declarations

Conflict of interest The authors declare no competing interests.

Ethical approval No permission was needed for this study.

References

Acebes-Doria AL, Agnello AM, Alston DG et al (2020) Season-long monitoring of the brown marmorated stink bug (Hemiptera: Pentatomidae) throughout the United States using commercially available traps and lures. J Econ Entomol 113:159–171. https://doi.org/10.1093/jee/toz240

Aldrich JR, Khrimian A, Camp MJ (2007) Methyl 2, 4, 6-decatrienoates attract stink bugs and tachinid parasitoids. J Chem Ecol 33:801–815. https://doi.org/10.1007/s10886-007-9270-9

Bariselli M, Bugiani R, Maistrello L (2016) Distribution and damage caused by *Halyomorpha halys* in Italy. EPPO Bull 46:332–334. https://doi.org/10.1111/epp.12289

Cambridge JE, Francoeur L, Hamilton GC (2017) Brown marmorated stink bug (Hemiptera: Pentatomidae) attraction to various light stimuli. Florida Entomol 100:583–588. https://doi.org/10.1653/024.100.0315

DeVoe RD, Souza de JM, Ventura DF (1997) Electrophysiological measurements of spectral sensitivities: a review. Braz J Med Biol Res 30(2):169–177. https://doi.org/10.1590/S0100-879X1997000200003

Egri Á, Kriska G (2019) How does the water springtail optically locate proper habitats? Spectral sensitivity of photo- and polarotaxis in *Podura aquatica*. J Exp Biol. https://doi.org/10.1242/jeb.199760

Egri Á, Farkas P, Bernáth B et al (2020) Spectral sensitivity of L2 biotype in the *Thrips tabaci* cryptic species complex. J Insect Physiol 121:103999. https://doi.org/10.1016/j.jinsphys.2019.103999

Endo N, Wakakuwa M, Arikawa K, Hironaka M (2014) Spectral preference in a free-flying condition of the southern green stink bug, *Nezara viridula* (Heteroptera: Pentatomidae). Jpn J Appl Entomol Zool 58:23–38. https://doi.org/10.1303/jjaez.2014.23

Endo N, Hironaka M, Honda Y, Iwamoto T (2022) Combination of UV and green light synergistically enhances the attractiveness of light to green stink bugs *Nezara* spp. Sci Rep 12:12279. https://doi.org/10.1038/s41598-022-16295-z

Faúndez EI, Rider DA (2017) The brown marmorated stink bug *Halyomorpha halys* (Stål, 1855) (Heteroptera: Pentatomidae) in Chile. Arquivos Entomolóxicos 17:305–307

Gingl E, Hinterwirth A, Tichy H (2005) Sensory representation of temperature in mosquito warm and cold cells. J Neurophysiol 94:176–185. https://doi.org/10.1152/jn.01164.2004

Govardovskii VI, Fyhrquist N, Reuter T et al (2000) In search of the visual pigment template. Vis Neurosci 17:509–528. https://doi.org/10.1017/S0952523800174036

Gribakin FG (1981) Automatic spectrosensitometry of photoreceptors in *Lethrus* (coleoptera, scarabaeidae). J Comp Physiol A 142:95–102. https://doi.org/10.1007/BF00605481

Hancock TJ, Lee D-H, Bergh JC et al (2019) Presence of the invasive brown marmorated stink bug *Halyomorpha halys* (Stål) (Hemiptera: Pentatomidae) on home exteriors during the autumn dispersal period: results generated by citizen scientists. Agric for Entomol 21:99–108. https://doi.org/10.1111/afe.12312

Haye T, Abdallah S, Gariepy T, Wyniger D (2014) Phenology, life table analysis and temperature requirements of the invasive brown marmorated stink bug, *Halyomorpha halys*, in Europe. J Pest Sci 87:407–418. https://doi.org/10.1007/s10340-014-0560-z

Hoebeke ER, Carter ME (2003) *Halyomorpha halys* (Stål) (Heteroptera: Pentatomidae): a polyphagous plant pest from Asia newly detected in North America. Proc Entomol Soc Wash 105:225–237

Jackowska M, Bao R, Liu Z et al (2007) Genomic and gene regulatory signatures of cryptozoic adaptation: loss of blue sensitive photoreceptors through expansion of long wavelength-opsin expression in the red flour beetle *Tribolium castaneum*. Front Zool 4:24. https://doi.org/10.1186/1742-9994-4-24

Kecskeméti S, Geösel A, Fail J, Egri Á (2021) In search of the spectral composition of an effective light trap for the mushroom pest *Lycoriella ingenua* (Diptera: Sciaridae). Sci Rep 11:12770. https://doi.org/10.1038/s41598-021-92230-y

Khrimian A, Shearer PW, Zhang A et al (2008) Field trapping of the invasive brown marmorated stink bug, *Halyomorpha halys*, with geometric isomers of methyl 2,4,6-decatrienoate. J Agric Food Chem 56:197–203. https://doi.org/10.1021/jf072087e

Khrimian A, Zhang A, Weber DC et al (2014) Discovery of the aggregation pheromone of the brown marmorated stink bug (*Halyomorpha halys*) through the creation of stereoisomeric libraries of 1-bisabolen-3-ols. J Nat Prod 77:1708–1717. https://doi.org/10.1021/np5003753

Lee D-H, Short BD, Joseph SV et al (2013) Review of the biology, ecology, and management of *Halyomorpha halys* (Hemiptera: Pentatomidae) in China, Japan, and the Republic of Korea. Environ Entomol 42:627–641. https://doi.org/10.1603/EN13006

Leskey TC, Nielsen AL (2018) Impact of the invasive brown marmorated stink bug in North America and Europe: history, biology, ecology, and management. Annu Rev Entomol 63:599–618. https://doi.org/10.1146/annurev-ento-020117-043226

Leskey TC, Hamilton GC, Nielsen AL et al (2012a) Pest status of the brown marmorated stink bug, *Halyomorpha halys* in the USA. Outlooks Pest Manag 23:218–226. https://doi.org/10.1564/23oct07

Leskey TC, Wright SE, Short BD, Khrimian A (2012b) Development of behaviorally-based monitoring tools for the brown marmorated stink bug (Heteroptera: Pentatomidae) in commercial tree fruit orchards. J Entomol Sci 47(1):76–85. https://doi.org/10.18474/0749-8004-47.1.76

Leskey TC, Lee D-H, Glenn DM, Morrison WR (2015) Behavioral responses of the invasive *Halyomorpha halys* (stål) (Hemiptera: Pentatomidae) to light-based stimuli in the laboratory and field. J Insect Behav 28:674–692. https://doi.org/10.1007/s10905-015-9535-z

Mazokhin-Porshnyakov GA, Cherkasov AD (1985) Spectral sensitivity of visual cells of the compound eye of *Blatta orientalis*. Neurophysiology 17:48–51. https://doi.org/10.1007/BF01052791

Morrison WR, Cullum JP, Leskey TC (2015) Evaluation of trap designs and deployment strategies for capturing *Halyomorpha halys* (Hemiptera: Pentatomidae). J Econ Entomol 108:1683–1692. https://doi.org/10.1093/jee/tov159

Mote MI, Goldsmith TH (1970) Spectral sensitivities of color receptors in the compound eye of the cockroach *Periplaneta*. J Exp Zool A Ecol Genet Physiol 173:137–145. https://doi.org/10.1002/jez.1401730203

Naka KI, Rushton WAH (1966) An attempt to analyse colour reception by electrophysiology. J Physiol 185:556–586. https://doi.org/10.1113/jphysiol.1966.sp008002

Nelder JA, Mead R (1965) A simplex method for function minimization. Comput J 7:308–313. https://doi.org/10.1093/comjnl/7.4.308

Nielsen AL, Holmstrom K, Hamilton GC et al (2013) Use of black light traps to monitor the abundance, spread, and flight behavior of *Halyomorpha halys* (Hemiptera: Pentatomidae). J Econ Entomol 106:1495–1502. https://doi.org/10.1603/EC12472

Polajnar J, Eriksson A, Lucchi A et al (2015) Manipulating behaviour with substrate-borne vibrations potential for insect pest control. Pest Manag Sci 71:15–23. https://doi.org/10.1002/ps.3848

Polajnar J, Maistrello L, Bertarella A, Mazzoni V (2016) Vibrational communication of the brown marmorated stink bug (*Halyomorpha halys*). Physiol Entomol 41:249–259. https://doi.org/10.1111/phen.12150

R Core Team (2022) R: a language and environment for statistical computing

Rice KB, Bergh CJ, Bergmann EJ et al (2014) Biology, ecology, and management of brown marmorated stink bug (Hemiptera: Pentatomidae). J Integr Pest Manage 5:A1–A13. https://doi.org/10.1603/IPM14002

Rondoni G, Chierici E, Marchetti E et al (2022) Improved captures of the invasive brown marmorated stink bug, *Halyomorpha halys*, using a novel multimodal trap. Insects 13:527. https://doi.org/10.3390/insects13060527

Schmitz A, SchAtzel H, Schmitz H (2010) Distribution and functional morphology of photomechanic infrared sensilla in flat bugs of the genus *Aradus* (Heteroptera, Aradidae). Arthropod Struct 39:15–25. https://doi.org/10.1016/j.asd.2009.10.007

Schmitz H, Soltner H, Bousack H (2012) Insect infrared sensors. In: Bhushan B (ed) Encyclopedia of nanotechnology. Springer, Dordrecht, pp 1110–1121. https://doi.org/10.1007/978-90-481-9751-4_263

Skorupski P, Chittka L (2010) Photoreceptor spectral sensitivity in the bumblebee, *Bombus impatiens* (Hymenoptera: Apidae). PLoS ONE 5:e12049. https://doi.org/10.1371/journal.pone.0012049

Sparks ME, Bansal R, Benoit JB et al (2020) Brown marmorated stink bug, *Halyomorpha halys* (Stål), genome: putative underpinnings of polyphagy, insecticide resistance potential and biology of a top worldwide pest. BMC Genomics 21:227. https://doi.org/10.1186/s12864-020-6510-7

Telles FJ, Lind O, Henze MJ et al (2014) Out of the blue: the spectral sensitivity of hummingbird hawkmoths. J Comp Physiol A 200:537–546. https://doi.org/10.1007/s00359-014-0888-0

Toyama M, Ihara F, Yaginuma K (2011) Photo-response of the brown marmorated stink bug, *Halyomorpha halys* (Stål) (Heteroptera: Pentatomidae), and its role in the hiding behavior. Appl Entomol Zool 46:37–40. https://doi.org/10.1007/s13355-010-0002-1

van der Kooi CJ, Stavenga DG, Arikawa K et al (2021) Evolution of insect color vision: from spectral sensitivity to visual ecology. Annu Rev Entomol 66:435–461. https://doi.org/10.1146/annurev-ento-061720-071644

Vétek G, Károlyi B, Mészáros Á et al (2018) The invasive brown marmorated stink bug (*Halyomorpha halys*) is now widespread in Hungary. Entomologia Generalis 38:3–14. https://doi.org/10.1127/entomologia/2018/0631

Virant-Doberlet M, Cokl A (2004) Vibrational communication in insects. Neotrop Entomol 33:121–134. https://doi.org/10.1590/S1519-566X2004000200001

Weber DC, Leskey TC, Walsh GC, Khrimian A (2014) Synergy of aggregation pheromone with methyl (E, E, Z)-2,4,6-decatrienoate in attraction of *Halyomorpha halys* (Hemiptera: Pentatomidae). J Econ Entomol 107:1061–1068. https://doi.org/10.1603/EC13502

Zapponi L, Nieri R, Zaffaroni-Caorsi V et al (2022) Vibrational calling signals improve the efficacy of pheromone traps to capture the brown marmorated stink bug. J Pest Sci. https://doi.org/10.1007/s10340-022-01533-0